



### Path to Plastics Composed of Ligninsulphonates (Lignosulfonates)

Journal:	<i>Green Chemistry</i>
Manuscript ID	GC-ART-08-2015-001865.R1
Article Type:	Paper
Date Submitted by the Author:	28-Aug-2015
Complete List of Authors:	Wang, Yun-Yan; University of Minnesota, Dept. of Bioproducts & Biosystems Engineering Chen, Yi-ru; University of Minnesota, Dept. of Bioproducts & Biosystems Engineering Sarkanen, Simo; University of Minnesota, Dept. of Bioproducts & Biosystems Engineering
<p>Note: The following files were submitted by the author for peer review, but cannot be converted to PDF. You must view these files (e.g. movies) online.</p> <p>scheme 1.cdx scheme 2.cdx</p>	



Journal Name

ARTICLE

## Path to Plastics Composed of Ligninsulphonates (Lignosulphonates)

Yun-Yan Wang, Yi-ru Chen and Simo Sarkanen\*

Received 00th January 20xx,  
Accepted 00th January 20xx

DOI: 10.1039/x0xx00000x

www.rsc.org/

The properties of lignin-based polymeric materials depend on blend composition and casting conditions. When solution-cast at 150° and annealed at 180°C, blends containing 85% w/w levels of methylated ball-milled softwood lignin can surpass polystyrene in tensile behaviour. It is more challenging to achieve similar results with comparable blends of ligninsulphonates, whether methylated or not. Nevertheless, 85% w/w ligninsulphonate-based materials containing miscible low- $T_g$  polymers can match the tensile properties of polyethylene. The ligninsulphonate components themselves are assembled into 9–15 nm macromolecular entities, the integrities of which are maintained through strong noncovalent interactions between inner co-facially disposed aromatic rings. In contrast, the peripheral aromatic rings typically exhibit a greater incidence of less stable edge-on arrangements. An intriguing aspect of the materials that are composed solely of (unmethylated or methylated) ligninsulphonates is their insolubility in water. This observation is consistent with the absence of a discernible glass-transition temperature in the differential scanning calorimetric thermograms of ligninsulphonate-based materials when they prominently display domains maintained by strong interactions between co-facial aromatic rings. The demonstrated integrity of polymeric materials composed (almost) exclusively of simple lignin derivatives has far-reaching implications for the configurations of lignin macromolecules in general. Contrary to an enduring hypothesis proposed 55 years ago, polymer chains in lignin preparations are not covalently crosslinked, even though their conformations are clearly affected by powerful noncovalent forces between the aromatic substructures.

### Introduction

Lignins are found in the cell-walls of all vascular plants; as a class, they represent the second most abundant group of biopolymers on earth. Lignin macromolecules possess as many as six different interunit linkages between *p*-hydroxyphenylpropane units. Depending on the origin of the lignin, the aromatic rings differ according to the substitution pattern of methoxyl groups (which are zero, one or two in number).<sup>1</sup> The substructures manifested along the lignin chains are distinguished with respect to the way in which the monomer units are linked to one another through either C–O or C–C single bonds. The resistance of these linkages to (bio)chemical cleavage accounts for the notorious recalcitrance of lignins. Indeed, the biodegradation of these imperfectly understood biopolymers is thought to uphold the rate-limiting step in the carbon cycle.<sup>2</sup>

The profitable conversion of lignocelluloses from plants to liquid biofuels and commodity organic chemicals depends on the value added to the co-product lignins.<sup>3</sup> The cleavage of such lignin derivatives to low-molecular-weight compounds may look like a reasonable possibility, but resistance to degradation and the broad range of products formed can dampen enthusiasm for such undertakings.<sup>4</sup> Alternatively, the prospect of converting lignin derivatives into useful polymeric materials will be improved by apprehending what kind(s) of configuration(s) best describe the

macromolecular species that are to be manipulated.<sup>5</sup>

Over half a century ago, the question of lignin configuration was considered from the perspective of the marked hydrodynamic compactness of ligninsulphonate macromolecules.<sup>6</sup> It was concluded that the small hydrodynamic volumes of these polyanions are consequences of intramolecular crosslinking between monomer residues along the macromolecular chains.<sup>6</sup> Later, in 1985, the delignification of softwood was analysed in terms of Flory-Stockmayer theory, whereby lignin dissolution was envisaged as a crosslinked-gel degradation process.<sup>7</sup> As recently as 2013, lignin macromolecules were described as hyper-branched polymer components in their capacity to act as a foundation for formulating polyurethane thermoplastics.<sup>8</sup>

Both unmodulated crosslinking and hyper-branching in macromolecular chains would result in rigid domains that require foreign soft segments (introduced chemically or by blending) to avoid undue brittleness in polymeric material formulations.<sup>9</sup> Unfortunately, such a strategy led to a 40% incorporation limit for lignins in plastics that has been almost insurmountable.<sup>10</sup>

There have, however, been occasional reports that expose a misunderstanding in the assumption that lignin macromolecules are crosslinked. The first promising formulations embodying 85% w/w softwood kraft lignin were described in 1997.<sup>11</sup> These materials consisted of kraft-lignin blends with poly(vinyl acetate) containing small quantities of diethyleneglycol dibenzoate and indene. The kraft lignin components had undergone self-assembly into macromolecular complexes (in response to strong intermolecular noncovalent forces), and the mechanical behaviour of the

Department of Bioproducts and Biosystems Engineering, University of Minnesota, Saint Paul, Minnesota, 55108-6120, United States, Email: sarka001@umn.edu



polymeric materials exhibited a marked dependence on the prevailing degree of association. The tensile strengths of the most promising formulations exceeded 25 MPa with a 5% elongation-at-break.<sup>11</sup> Results at this level are not far removed from the corresponding values<sup>12</sup> for polyethylene (30 MPa, 9% elongation-at-break).

Eight years later, further improvements in tensile strength had been recorded for various homogeneous blends of alkylated softwood kraft lignin preparations.<sup>13</sup> For example, a methylated high-molecular-weight kraft lignin fraction blended with 20% poly(ethylene glycol) was found to possess a tensile strength of 49 MPa with 7% elongation-at-break. Such tensile behaviour surpasses that of polystyrene.<sup>12</sup> An eloquent correlation was observed between the glass transition temperature ( $T_g$ ) and mechanical behaviour of alkylated kraft lignin-based blends with aliphatic polyesters as they were altered by blend composition.<sup>14</sup> The correlation was consistent with the previous realization that the individual kraft lignin components are assembled into macromolecular complexes<sup>11</sup> as a result of strong intermolecular noncovalent interactions.<sup>15</sup>

No crystallinity has ever been reported in materials composed of lignins or simple lignin derivatives. However, X-ray powder diffraction analyses have provided evidence for two distinct series of arrangements that can characterize interacting aromatic rings in polymeric materials with very high lignin contents. Thus, the diffuse X-ray scattering from methylated paucidisperse kraft lignin fractions has been described as a sum of two broad Lorentzian peaks centred at equivalent Bragg spacings ( $d$ ) of  $\sim 4.0$  Å and  $\sim 5.2$  Å.<sup>13</sup> From a comparison with the average  $d$ -spacings between co-facial and edge-on aromatic rings in the crystal structures of lignin-model compounds, the respective Lorentzian peaks were attributed to these two contrasting arrangements of interacting aromatic rings in associated lignin complexes. Presumably the co-facial aromatic rings are predominantly located within the interiors of the macromolecular entities, while the edge-on configurations would be expected largely to occupy the peripheral regions. Such flexibility in arrangement for the interacting aromatic rings may be necessary in some instances to establish continuity between adjacent complexes in lignin-based polymeric materials.

Although the Kraft process is the operation pre-eminently employed for the chemical pulping of wood, the resulting co-product lignins currently have limited commercial value. Thus, sulphite pulping should be considered as an alternative source of lignin derivatives for producing useful polymeric materials. The conversion of water-soluble polyanionic ligninsulphonates into thermoplastics could be challenging, but the Borregaard wood-based biorefinery in Sarpsborg (Norway) is designed to produce

160,000 tonnes of such co-product lignins annually.<sup>16</sup> For reference purposes in the exploratory studies described here, a comparison has been made between a methylated ball-milled lignin and a softwood ligninsulphonate as alternative starting materials for formulating plastics with very high lignin contents.

Over the past 30 years, lignin preparations have been incorporated into numerous copolymers, blends and composites.<sup>10,17</sup> Although only considered infrequently, polymeric materials containing simple lignin derivatives at >70% levels could provide important insight into what would be the most effective means of valorising co-product lignins. Accordingly, this is the focus of the first study devoted to developing formulations for ligninsulphonate-based materials.

## Results and discussion

The ball-milled lignin (BML) in 18% yield was isolated from Jack pine (*Pinus banksiana*) and purified according to Lundquist's protocol.<sup>18</sup> Its weight- and number-average molecular weights were determined size-exclusion chromatographically to be 4300 and 1850, respectively, under conditions that have been previously described.<sup>13, 14</sup> No detectable monosaccharides were released from this preparation as a result of acid-catalysed hydrolysis.<sup>19</sup> The quantitative <sup>13</sup>C-NMR spectrum (Fig. 1A) of the BML (as a 20% solution in DMSO- $d_6$ ) was very similar to that previously reported for spruce milled wood lignin.<sup>20</sup> The  $\delta_c$  55.6 ppm C-3 methoxyl peak area, when multiplied by 6.12,<sup>20</sup> amounted to 99.3% of the spectral area in the aromatic range ( $\sim 108$ – $156$  ppm), indicating that the BML was composed almost entirely of guaiacyl units.

After consecutive methylation with dimethyl sulphate and diazomethane, the proportion of aromatic methoxyl groups (centred around 55.5 and 56.6 ppm) increased by 31% (Fig. 1B) owing to the manifestation of these groups on C-4 of the methylated ball-milled lignin (MBML). This increase is identical to the estimated phenolic hydroxyl group frequency in spruce milled wood lignin.<sup>20</sup> The effect is consistent with the observed shift of a conspicuous portion of the  $\delta_c$  147.4 aromatic C-4 BML feature to 148.5 ppm in the MBML (Fig. 1C).

Methylation also gave rise to aliphatic methoxyl signals centred around  $\delta_c$  58.5 with a  $\sim 4$ -fold smaller peak appearing at 58.2 ppm (Fig. 1B); together these amounted to an area equivalent to 31% of the original aromatic C-3 methoxyl substituents. These aliphatic methoxyl groups are bound, in part, to C- $\gamma$  of  $\beta$ -O-4 ethers, and indeed the corresponding C- $\beta$  around  $\delta_c/\delta_H \sim 84.3/4.3$  in the HSQC spectrum of BML shifted to  $\delta_c/\delta_H$  82.3/4.4 after methylation (Fig. 1D).

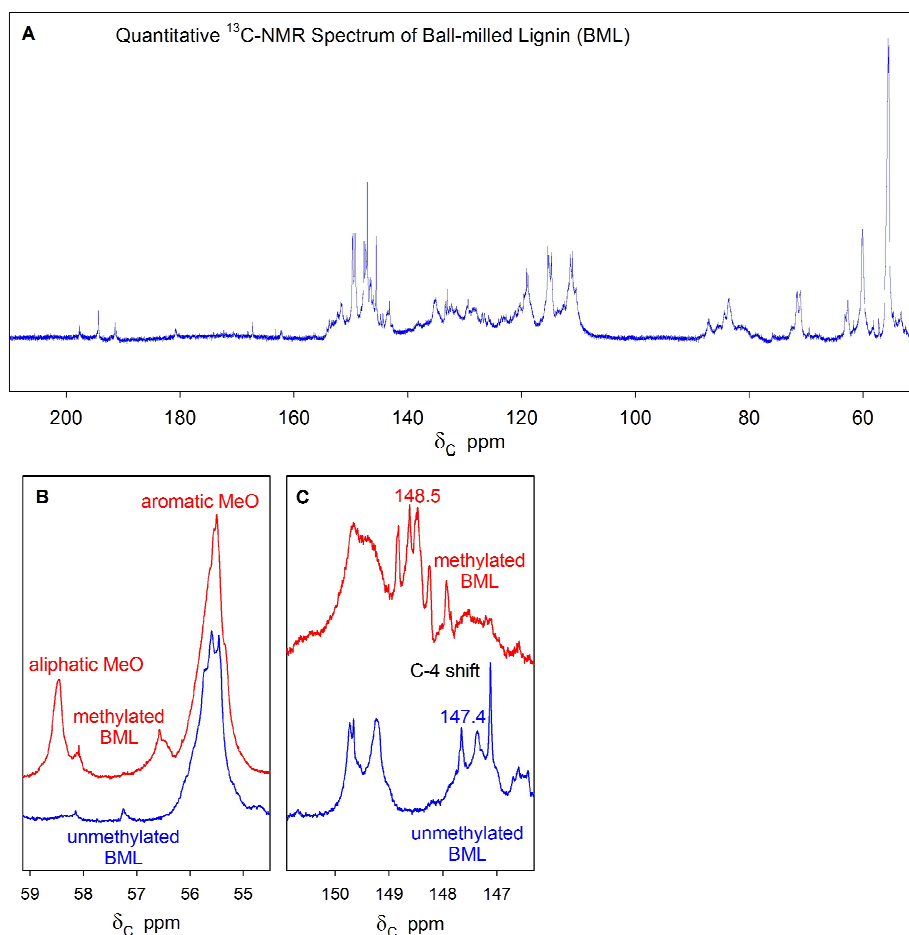


**Fig. 1** Quantitative  $^{13}\text{C}$ -NMR spectral intervals of underivatized and methylated ball-milled Jack pine lignin (BML) in  $\text{DMSO-}d_6$ . (A) 50–210 ppm interval of underivatized BML; (B) 54.5–59 ppm interval circumscribing methoxyl region of underivatized and methylated BML; (C) 146.5–150.5 ppm interval encompassing C-4 in underivatized and methylated BML; (D) HSQC spectral region enclosing C- $\beta$  of alkyl aryl ether in underivatized and methylated BML

All formulations for the lignin-based polymeric materials described below were solution cast using DMSO as solvent. The blend-compositions were chosen to create an initial framework for the materials being compared. As far as methylated ball-milled lignin-based materials are concerned, the casting conditions have a significant effect on tensile behaviour: in the absence of other blend components, the more volatile lignin-derived oligomers (produced under the lignin-isolation conditions themselves) act as plasticizers. When cast at 150 °C, the methylated ball-milled lignin (MBML) alone exhibits a tensile strength of 43 MPa with 5% elongation-at-break (Fig. 2). Such a result compares very favourably with polystyrene (46 MPa, 2.2% elongation-at-break<sup>12</sup>) and clearly refutes the likelihood of crosslinking in lignins. All of the phenolic and many of the aliphatic hydroxyl groups in the ball-milled lignin are methylated under the derivatization conditions employed (*vide supra*); this simple step reduces the brittleness of the cast materials substantially. Blending of MBML with 15% poly(ethylene glycol) leads to a tensile strength of 52 MPa with elongation-at-break above 6%.

However, 15% levels of poly(ethylene oxide-*b*-1,2-butadiene) or poly(trimethylene glutarate) do not individually improve the tensile behaviour of 85% MBML-based polymeric materials (Fig. 2).

Calcium bisulphite pulping of Douglas fir forest-harvest residuals was carried out for 6 h at 145 °C in the presence of 6.6% (w/w) total  $\text{SO}_2$  (with respect to wood) under conditions previously described.<sup>21</sup> The purity of the ligninsulphonate in the spent liquor was increased 2-fold by consecutive ultrafiltration through 200 kDa and 4 kDa nominal molecular weight cutoff membranes. The resulting 87% pure ligninsulphonate held in the 4 kDa-membrane retentate was employed to develop formulations for polymeric materials with high ligninsulphonate contents. By means of size-exclusion chromatography, this polyanionic lignin derivative was found to possess weight- and number-average molecular weights of 23.4 and 12.9 kDa; its reported S content was consistent with an average sulphonation frequency of 0.48 per monomer unit.<sup>21</sup>

The ligninsulphonate (LS) was methylated either with dimethyl sulphate alone or consecutively with dimethyl sulphate and diazomethane. The peak-areas in the quantitative  $^{13}\text{C}$ -NMR spectra (Fig. 3) of the singly and doubly methylated derivatives (sMLS and dMLS as 20% and 10% solutions, respectively, in  $\text{DMSO-}d_6$ ) were scaled in relation to the corresponding aromatic spectral features (107–156 ppm) in keeping with the protocol for the BML and MBML analyses

result of subsequent methylation by diazomethane, whereupon the  $\delta_c$  55.5 peak-ratio rose to 1.45 (Fig. 3). Reaction of sMLS with diazomethane also raised the frequency of aliphatic methoxyl groups in dMLS: the relative area of the signal centred around  $\delta_c$  58.4–58.5 ppm increased from 0.19 to 0.30 (Fig. 3). Interestingly, this final value for dMLS is almost identical to the corresponding ratio for MBML (*vide supra*).

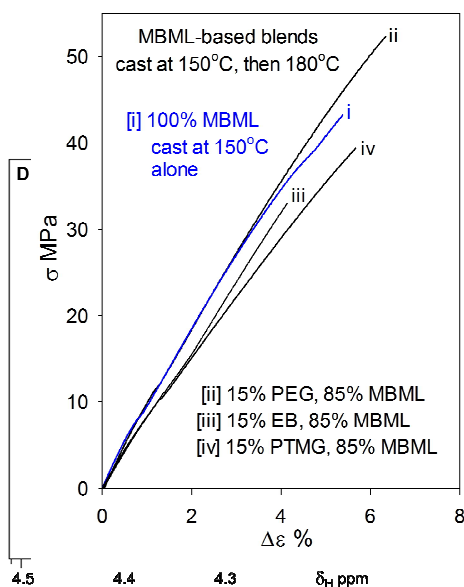


**Fig. 2** Tensile behaviour of methylated ball-milled lignin (MBML)-based polymeric materials. [i] 100% MBML-based plastic; blends of 85% MBML with [ii] 15% poly(ethylene glycol) (PEG), [iii] 15% poly(ethylene oxide-*b*-1,2-butadiene) (EB) and [iv] 15% poly(trimethylene glutarate) (PTMG).

(*vide supra*). After multiplying the overall  $\delta_c$  55.5 peak-area by 6.12,<sup>20</sup> it was evident that the C-3 and C-4 methoxyls<sup>22</sup> along with the methyl sulphonate groups<sup>23</sup> in the sMLS contributed, on average, 1.39 methyl groups altogether to each sMLS monomer unit (Fig. 3). Comparison with the corresponding ratio for MBML here reveals that a substantial number of the sulphonic acid groups had already been methylated by dimethyl sulphate. This proportion increased significantly as a

result of subsequent methylation by diazomethane, whereupon the  $\delta_c$  55.5 peak-ratio rose to 1.45 (Fig. 3). Reaction of sMLS with diazomethane also raised the frequency of aliphatic methoxyl groups in dMLS: the relative area of the signal centred around  $\delta_c$  58.4–58.5 ppm increased from 0.19 to 0.30 (Fig. 3). Interestingly, this final value for dMLS is almost identical to the corresponding ratio for MBML (*vide supra*).

Casting the singly-methylated ligninsulphonate (sMLS) alone resulted in a material that exhibits a 28 MPa tensile strength with 5% elongation-at-break (Fig. 4). An outcome like this suggests that certain simple sMLS blends should be capable of matching polyethylene (30 MPa strength with 9% elongation-at-break) in their tensile behaviour.<sup>12</sup> However, a sMLS-based material cast with 15% w/w poly(trimethylene glutarate) suffered a >10% reduction in tensile strength, although the corresponding blend with 15% w/w polycaprolactone supported a 40% improvement in elongation-at-break (Fig. 4).

A particularly interesting result was encountered with the doubly-methylated ligninsulphonate (dMLS). A dMLS-based blend with 15% w/w poly(trimethylene glutarate) manifested a 24 MPa tensile strength with 11% elongation-at-break (Fig. 4). Evidently, the reduction in intermolecular hydrogen bonding that accompanies complete phenolic hydroxyl and sulphonic-acid group methylation can reduce the brittleness of certain ligninsulphonate-based polymeric material blends quite appreciably.

The impact of the various noncovalent forces (hydrogen bonding, electron correlation, dipolar interactions) on the ductility of LS-based materials is difficult to predict in reference to any particular blend composition. For example, an unmethylated LS-based blend with 15% w/w poly(trimethylene glutarate) has manifested a tensile strength near 35 MPa with 7% elongation-at-break, even though the solution-cast material based on LS alone did not exceed 22 MPa in tensile strength with 3.5% elongation-at-break (Fig. 5). Yet, the corresponding LS-based blends with 15% w/w polycaprolactone and 15% poly(trimethylene succinate) individually exhibited tensile strengths of 26 and 30 MPa, respectively, at 5% and 6% elongations-at-break (Fig. 5).

The arrangements of the aromatic rings among chain segments in the unmethylated and methylated LS-based materials are reflected in their X-ray powder diffraction patterns. Before and after casting, the diffuse scattered intensities may be typically described as sums of two overlapping Lorentzian peaks with maxima centred at equivalent Bragg spacings ( $d$ ) of 3.9 – 4.2 Å and 5.8 – 6.1 Å (Figs. 6A–F). In accordance with previous X-ray powder diffraction analyses of paucidisperse kraft lignin fractions,<sup>13</sup> the two distributions of separation distances can be respectively attributed to distinct series of co-facial and edge-on arrangements of interacting aromatic rings. The contributions to the decrease in energy from the noncovalent forces that stabilize the two kinds of configurations have been estimated to be 7 – 11 and ~4 kcal/mol, respectively, at the M05-2X/6-31+G(d,p) level of density of functional theory.<sup>15</sup>

The co-facial arrangements of interacting aromatic rings presumably occupy the inner regions of the macromolecular entities in the unmethylated and methylated LS, while the edge-on orientations are more prevalent among the peripheral chain segments. In the cast materials, the proportions of the two contrasting configurations of interacting aromatic rings are determined, in part, by the requirements for continuity between adjoining macromolecular species. There is a notable decrease in the proportion of edge-on arrangements of aromatic rings as a direct result of casting all three LS-based materials (Figs. 6A–F). In the case of the unmethylated LS, the Lorentzian peak emanating from the edge-on configurations disappeared altogether during casting. Evidently, the contours of the stable co-facial arrangements of aromatic rings in the

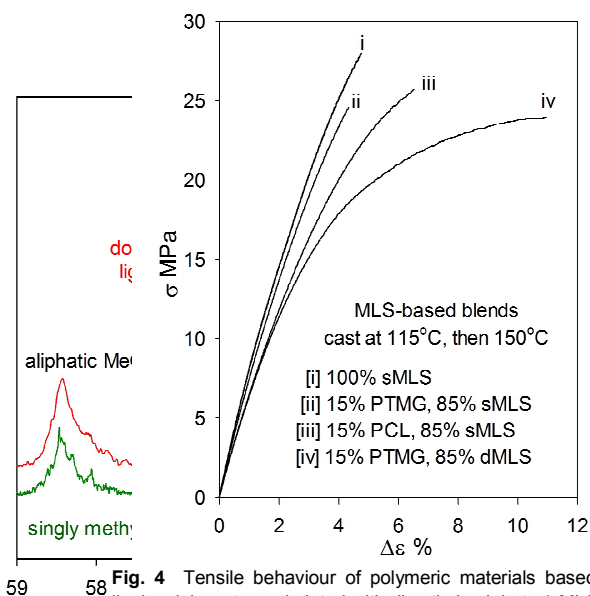


**Fig. 4** Tensile behaviour of polymeric materials based on ligninsulphonate methylated with dimethyl sulphate (sMLS) or dimethyl sulphate followed by diazomethane (dMLS). [i] 100% sMLS; blends of 85% sMLS with [ii] 15% PTMG, 85% sMLS; [iii] 15% PCL, 85% sMLS; [iv] 15% PTMG, 85% dMLS.

**Fig. 3** Quantitative XRD analysis of the methoxyl region of poly(trimethylene glutarate) (PTMG) and [iii] 15% dimethyl sulphate polycaprolactone (PCL); [iv] blend of 85% dMLS with 15% PTMG cast stepwise at 115°, 125°, 135° and then 150°C.

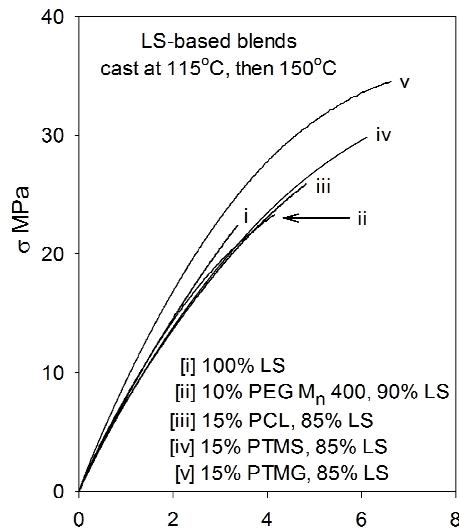


**Fig. 5** Tensile behaviour of ligninsulphonate (LS)-based polymeric materials. [i] 100% LS; [ii] blend of 90% LS with 10% PEG,  $M_n$  400 Da; blends of 85% LS with [iii] 15% polycaprolactone (PCL), [iv] 15% poly(trimethylene succinate) (PTMS), and [v] 15% poly(trimethylene glutarate) (PTMG).

cast material can match one another without the persistence of Å- or nm-scale voids between

adjacent macromolecular entities. Fresh surfaces of the cast unmethylated and methylated LS-based materials were created by ultramicrotome-cutting with a 45° glass blade. The procedure was carried out (between ambient and -60°C) at a temperature above which the surface features showed some likelihood of coalescing or otherwise undergoing deformation. Atomic force microscopy (AFM) was employed in the tapping mode to probe the surfaces of the three cast (LS, sMLS and dMLS) materials represented in terms of the respective tip-oscillation amplitude images (Figs. 7A–C) and, for confirmatory purposes, the corresponding height images (exemplified in Fig. 7D).

Adjacent local maxima in the nodular surface features of the LS-, sMLS- and dMLS-based materials are separated by  $12.2 \pm 3.2$ ,  $16.7 \pm 4.3$  and  $20.3 \pm 5.5$  nm, respectively. These distances mirror the ranges of the effective diameters characterizing the macromolecular entities of which the unmethylated and methylated LS-based materials are composed. It is unlikely that LS-methylation would engender covalent formation of larger macromolecular entities, and thus the increase in diameter of these species is more likely to arise from coalescence during casting. The probability of coalescence rests on the molecular-weight dependence of the intermolecular interactions between the individual LS components. In this respect, it seems that the macromolecular entities in the cast sMLS- and dMLS-based materials are (in three dimensions) 2.17- and 3.98-fold larger, respectively, than those making up the unmethylated LS. Such a situation could occur, for example, if the strongest noncovalent interactions between the methylated LS components were to involve the intermediate rather than higher chain lengths.

The question naturally arises as to whether the dimensions of the constituent macromolecular entities in the cast unmethylated and methylated LS-based materials are reasonable in relation to any previous estimates. A 2010 study of the track-etched-membrane fractionation of an industrial kraft lignin sample at  $0.01 \text{ gL}^{-1}$  in aqueous solution concluded that over 60% and 70%, respectively, of the supra-macromolecular solute species were below 30 nm in size at pHs 7.0 and 9.5.<sup>24</sup> The similarity of these results to those presently reported for LS-based materials is particularly striking because the supra-macromolecular kraft lignin species had undergone expansion as a result of their dissolution/suspension in aqueous solution.

In relation to the actual surface topologies of the LS-based materials, the AFM images in Fig. 7 have been convoluted in regard to the smoother traces produced with the  $<10 \text{ nm}$  tip radius of the instrument probe.<sup>25</sup> This limitation will not, however, impose an appreciable error on the values of the separation distances between peak maxima.

## Experimental description

### Ball-milled lignin isolation and methylation

Jack pine 1.5 cm<sup>3</sup> saw wood blocks were ground in a Wiley mill to a 40-mesh particle size. The resulting wood meal was Soxhlet-extracted with acetone for 48 h. The dry extractive-free wood meal was then milled in a cooled vibratory ball mill under N<sub>2</sub> for 48 h. A 40 g quantity of the

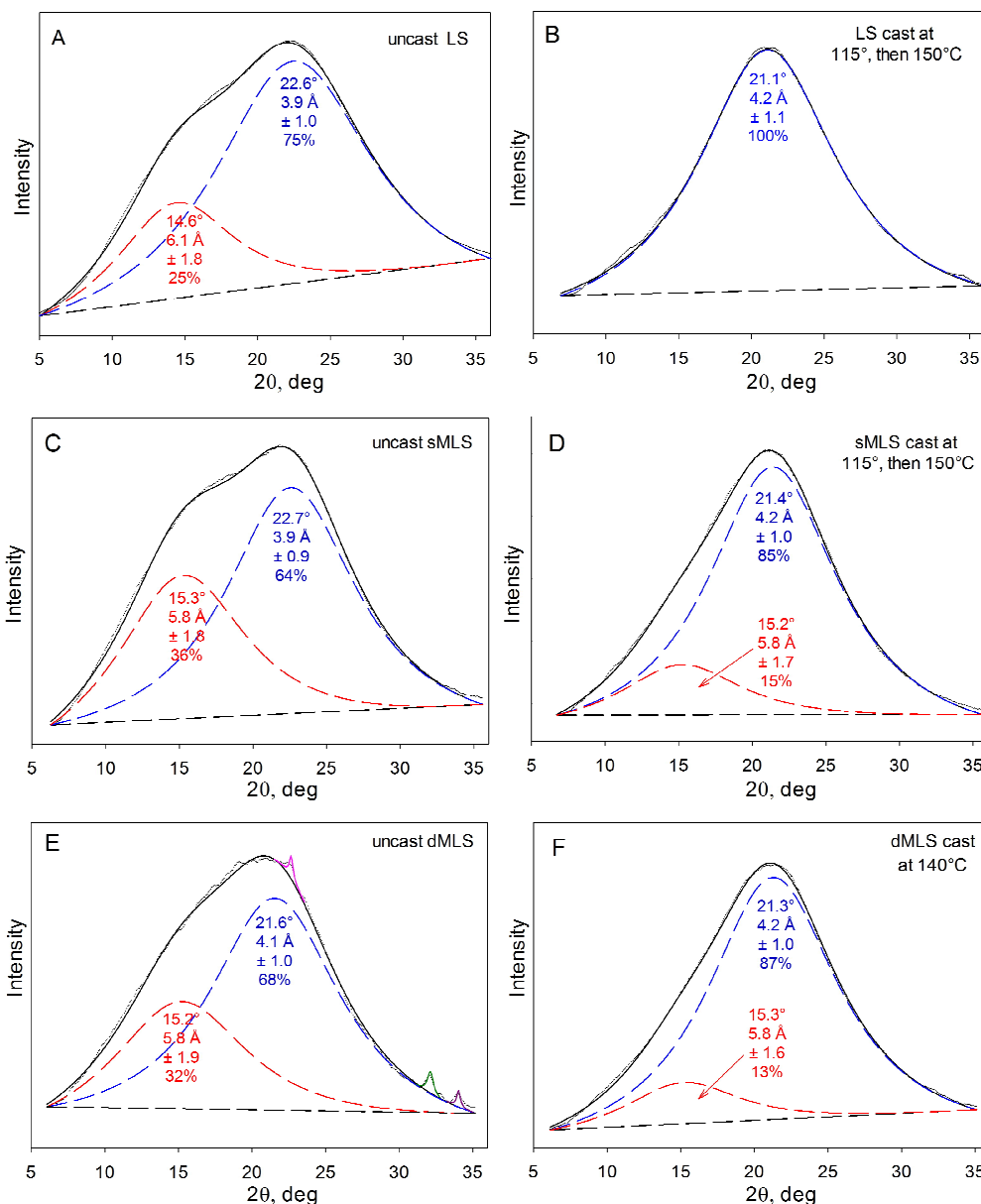


**Fig. 6** X-ray powder diffraction patterns of uncast and cast polymeric materials based on unmethylated and methylated ligninsulphonates. (A) uncast and (B) cast unmethylated ligninsulphonate (LS); (C) uncast and (D) cast ligninsulphonate methylated with dimethyl sulphate (sMLS); (E) uncast and (F) cast ligninsulphonate successively methylated with dimethyl sulphate and diazomethane (dMLS). The x-ray diffraction patterns of the amorphous polymeric materials were analysed by fitting two Lorentzian functions  $I(x) = I(0)/(1 + x^2/hw^2)$ ,  $x = 2\theta - 2\theta_k$ , where  $I(x)$  is the scattered intensity at  $x$  from the Bragg angle  $2\theta_k$  for the peak,  $2\theta$  is the scattering angle, and  $hw$  is the half-width at the half-maximum of the peak.

ball-milled wood meal was suspended and stirred in dioxane–water (96:4 v/v) three consecutive times over 96 h. The extracts were centrifuged (3000 rpm, Beckman J6B, 30 min) and thereafter the solvents were removed by rotary evaporation. The lignin isolated (in 18% yield) was purified by treatment with 9:1:4:18 v/v/v/v pyridine/acetic acid/water/chloroform whereupon, after solvent removal, the remaining material was dissolved in 2:1 v/v dichloroethane/ethanol and precipitated with ether.<sup>18</sup> The

carbohydrate content of the resulting product was so low that any monosaccharides liberated through acid catalysis could not be detected by standard chromatographic means.

The purified ball-milled lignin sample was methylated (Scheme 1) with dimethyl sulphate (Sigma-Aldrich) in alkaline aqueous dioxane solution and then with diazomethane in chloroform, as previously described for softwood kraft lignins.<sup>13,14</sup>



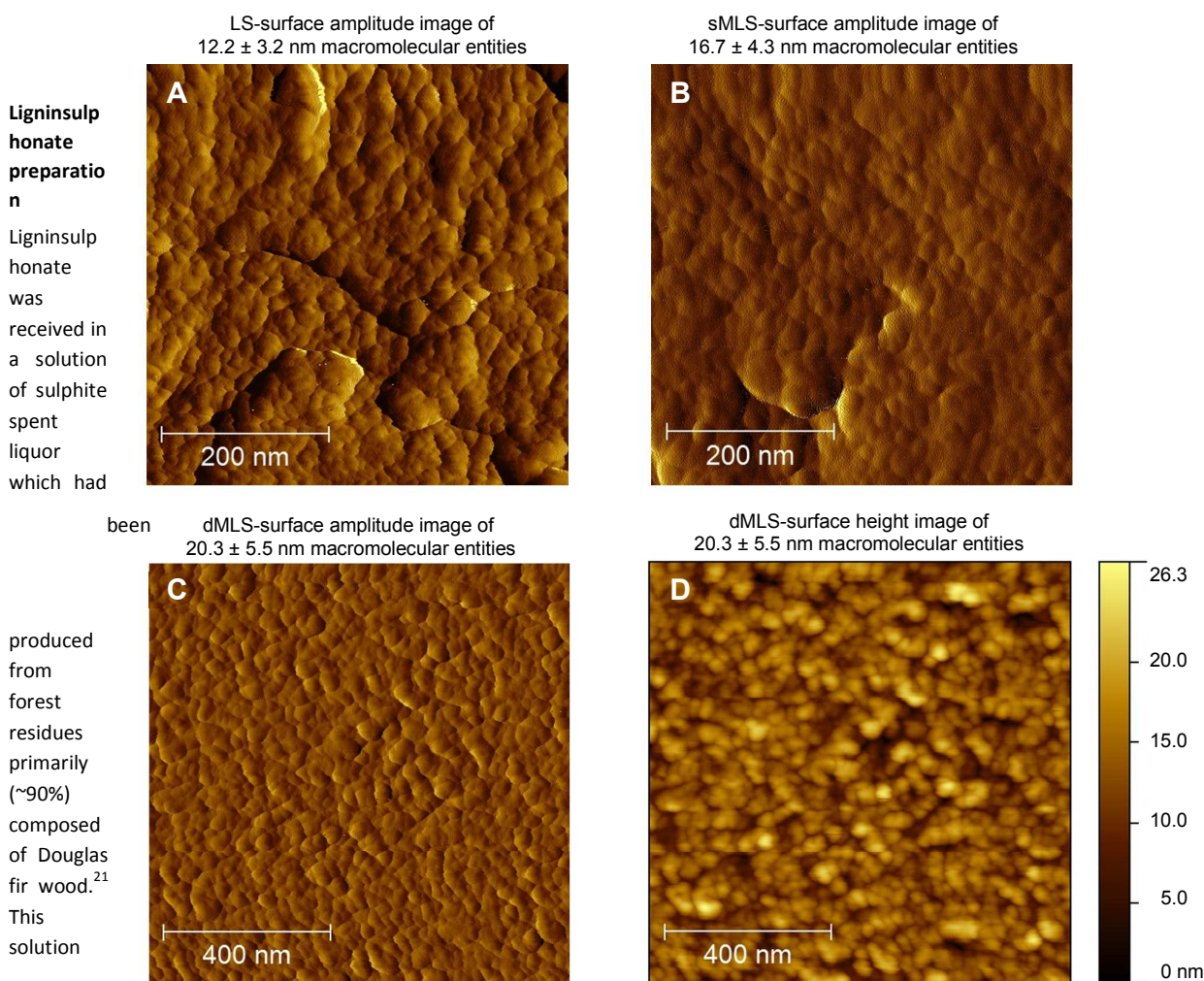
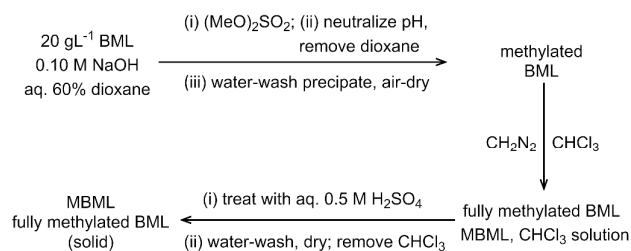


**Fig. 7** Packing of macromolecular entities in ligninsulphonate (LS)-based polymeric materials cast at 115° and then 150°C. Tapping-mode AFM amplitude images of ultramicrotome-cut surfaces of (A) unmethylated LS, (B) LS methylated with dimethyl sulphate (sMLS), (C) LS successively methylated with dimethyl sulphate and diazomethane (dMLS); (D) corresponding height image of dMLS surface (material cast stepwise at 115°, 125° and 150°C).



**Scheme 1** Laboratory methylation of ball-milled lignin (BML)

had been ultrafiltered through a 200 kDa nominal-molecular-weight-cutoff membrane and retained by a 4 kDa membrane before shipment. Ligninsulphonate samples were prepared by exhaustive ultrafiltration in water through a 1 kDa nominal-molecular-weight-cutoff membrane followed by freeze-drying of the solution with pH adjusted to 7.5. Prior to further processing, the ligninsulphonate was protonated with Amberlite IR120 (Sigma-Aldrich) in methanol<sup>26</sup>

which, after filtration, was subsequently removed by rotary evaporation.

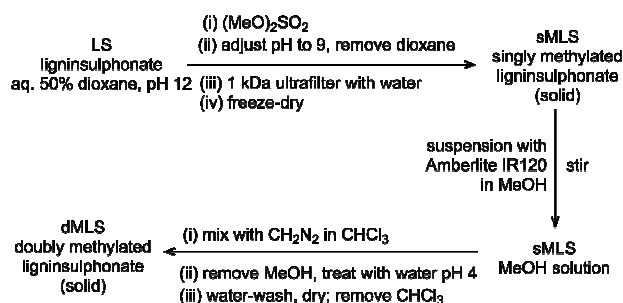
#### Methylation of ligninsulphonate with dimethyl sulphate

A quantity of 3.6 g ligninsulphonate in 600 mL aqueous 50% dioxane was methylated with 25 mL dimethyl sulphate (Sigma-Aldrich) at pH ~13. The pH of the mixture kept falling as a result of hydroxyl-group methylation. A solution containing 4.0 M NaOH and a corresponding amount of dioxane were repeatedly added to maintain the pH of the mixture at a value between 12.5 and 13.5. When the pH remained constant upon basification, the same amount of dimethyl sulphate was again added. This overall procedure was repeated 4 times. When the reaction was deemed complete, the solution mixture was neutralized with aqueous 0.1 M H<sub>2</sub>SO<sub>4</sub>. The dioxane was removed by rotary evaporation, whereupon the resulting solution was subjected to ultrafiltration in water through a 1 kDa nominal-molecular-weight-cutoff

membrane. After brief centrifugation to remove traces of insoluble material, the retentate was freeze-dried (Scheme 2).

### Methylation of methylated ligninsulphonate with diazomethane

About 1.8 g partially methylated ligninsulphonate was protonated using Amberlite IR120<sup>26</sup> in ~150 mL methanol before the sulfonic acid groups were methylated in chloroform with diazomethane prepared as previously described.<sup>13,14</sup> The reaction mixture was allowed to proceed in the dark for ~16 h, and the entire procedure was repeated until methylation was complete. The volume of the reaction mixture (~2 L) was reduced to ~500 mL by rotary evaporation. About 300 mL acidified water (pH 4.1) was introduced to discharge any residual diazomethane. After exhaustive washing with distilled water, the methylated ligninsulphonate solution was dried with sodium sulphate, and the chloroform removed under reduced pressure (Scheme 2).



### Size-exclusion chromatography (SEC)

**Scheme 2** Laboratory methylation of ligninsulphonate (LS)

The molecular weight distribution of BML was determined by eluting through Sephadex G100 (Sigma-Aldrich) in aqueous carbonate-free 0.10 M NaOH. The SEC profile was monitored spectrophotometrically at  $A_{280}$  and calibrated with paucidisperse poly(styrene sulphonate) fractions (American Polymer Standards, Mentor, OH). The elution profile exhibited no excluded peak (Fig. 8). The weight- and number-average molecular weights of LS were determined under conditions that have been previously described.<sup>21</sup>

### NMR analysis

Quantitative <sup>13</sup>C NMR spectra were recorded with a 600 MHz Varian Inova instrument using a 5 mm HCN cold probe. Weights amounting to ~0.2 g BML, MBML and sMLS were individually dissolved in 1 g DMSO-*d*<sub>6</sub>, while ~0.1 g dMLS was similarly dissolved in the same solvent. A 90° pulse width, 1.4 s acquisition time and 12 s relaxation delay were employed in collecting 10,000 scans from each solution. Chemical shifts were referenced to DMSO (39.51 ppm). The 2D Q-HSQC spectra<sup>27</sup> of BML and MBML were obtained from 5% solutions in DMSO-*d*<sub>6</sub> using a 700 MHz Bruker Avance instrument with a 5 mm TXI cryoprobe.

### Solution casting

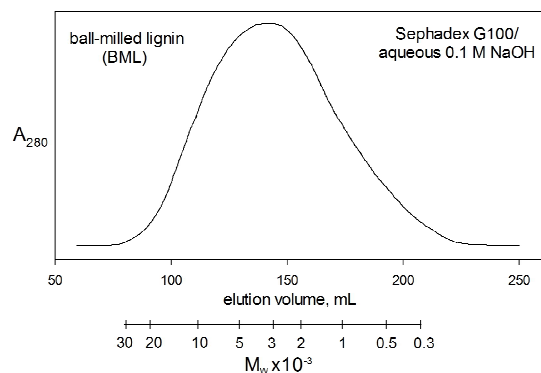
A 0.6 g quantity of ball-milled lignin or ligninsulphonate with or without other blend components was dissolved in 4.0 mL dimethyl sulphoxide (DMSO) in a 10 x 20 mm Teflon mould at 50° or 80°C, respectively. After degassing under reduced pressure in a vacuum oven at 50°C for 15 min, the ball-milled lignin test pieces were produced by solution-casting at 150° for a day and then 180°C for 3 h. The ligninsulphonate-based blend-component solutions were degassed in a similar way at 80°C for 15 min, and the corresponding test pieces were formed by solution-casting typically at 115°C for 24 h and then 150°C for a further 24 h.

### Tensile tests

The solid rectangular test pieces were filed into dog-bone-shaped specimens of which the typical dimensions were 5 mm in width, 8 mm in length between shoulders and ~1 mm in thickness. The tensile behaviour of each ligninsulphonate-based plastic specimen was characterized by means of a stress-strain curve measured with an Instron model 5542 unit fitted with a 500 N static load cell. Serrated jaws were used to hold all test pieces in place. No tensile test was initiated until the load reading had become stable. A crosshead speed of 0.05 mm min<sup>-1</sup> was employed with specimen gauge lengths of 7~8 mm. Young's modulus (*E*) and the stress ( $\sigma_{max}$ ) and strain ( $\epsilon_{\sigma,max}$ ) at fracture were calculated on the basis of initial sample dimensions.

### Differential scanning calorimetry (DSC)

DSC measurements were performed with a Q2000 instrument (TA Instruments) equipped with Refrigerated Cooling System 90. Samples weighing ~8 mg were sealed with a lid in an aluminium pan after flushing with N<sub>2</sub> for 15 h in a glove-box. Each unmethylated or singly-methylated ligninsulphonate preparation was pre-scanned from 40° to 170°C at 10°C min<sup>-1</sup>. The second scan was carried out



from -90° to 165°C at a heating rate of 10°C min<sup>-1</sup>. The glass-transition temperature would have been identified as the half-height point in the glass-transition region of the DSC thermogram,

**Fig. 8** Molecular weight distribution of ball-milled Jack pine lignin ( $M_w = 4300$ ,  $M_n = 1850$ ). Aqueous 0.1 M NaOH/Sephadex G100 elution profile calibrated by paucidisperse poly(styrene sulphonate) fractions.



had the requisite feature been present.

### X-ray powder diffraction

X-ray diffraction patterns were obtained in a  $5^\circ - 36^\circ$  range of the diffraction angle,  $2\theta$  (where  $\theta$  is the angle of the  $1.542 \text{ \AA}$  incident beam), with a Bruker AXS D5005 diffractometer operating in the reflection mode using  $\text{Cu K}\alpha$  radiation and a diffracted-beam monochromator. Powdered unmethylated and methylated ligninsulphonate samples were compressed onto a zero-background holder and  $0.06^\circ$  step-size scans were taken with 18 s dwell times. The diffraction patterns generated by these amorphous unmethylated and methylated ligninsulphonates (Fig. 4) were fitted to sums of two Lorentzian functions<sup>28</sup> with respect to a fixed algebraic baseline identified for each complete pattern to lie below that for the experimental data. The contributions from the two peaks to any overall diffraction pattern are consequently proportional to the Lorentzian peak-area sections above the experimental baseline.

### Atomic force microscopy (AFM)

After sectioning and trimming, the unmethylated and methylated ligninsulphonate-based materials were individually mounted in a specimen-holder fitted with a double-D clamp (Mager Scientific, Dexter, MI). The surface of each specimen was smoothed using a  $45^\circ$  glass blade for ultramicrotome-cutting with a  $1 \mu\text{m}$  step-size on a Leica EM UC6 apparatus to produce successive layers. The resulting surface was burnished further, using a  $100 - 300 \text{ nm}$  step-size several times, and immediately subjected to AFM scanning. The AFM experiments were carried out with a Bruker Nanoscope V multimode 8 scanning-probe microscope employed in a tapping mode for generating tip-oscillation-amplitude images. The monolithic silicon probe (Arrow<sup>TM</sup> NCR, NanoWorld AG, Switzerland) chosen for this work featured a  $160\text{-}\mu\text{m}$ -long cantilever holding a tetrahedral tip  $10 - 15 \mu\text{m}$  in height with a typical radius of curvature less than  $10 \text{ nm}$ . AFM scans were recorded with a Nanoscope 8.15 unit (Bruker) while online plane-fitting for images was turned off. Gwyddion software<sup>29</sup> was used to process and analyse the AFM images. The centre-to-centre distances between adjacent nodular features in the amplitude images (Fig. 5A–C) were measured manually.

### Conclusions

The first comparative survey of unmethylated and methylated ligninsulphonate-based polymeric materials has been carried out. The new materials are composed of macromolecular entities with  $9 - 15 \text{ nm}$  dimensions. Simple blends with small quantities ( $<15\%$ ) of miscible low- $T_g$  polymers can match polyethylene in tensile behaviour. Such findings are promising.

There are two notable aspects to the properties of the unmethylated and singly-methylated ligninsulphonate-based materials. First, their differential scanning calorimetric thermograms are without features that could be related to a glass-transition temperature. Evidently the prominent domains that encompass co-facially disposed aromatic rings

among the constituent macromolecular species (Fig. 4) cannot accommodate sufficient chain-segmental motion.

Second, the unmethylated and singly-methylated ligninsulphonate-based materials do not, after casting, dissolve in water despite the original solubility of the components in aqueous solution. Thus, pronounced physicochemical changes have taken place at elevated temperatures that have either dramatically increased the  $\text{pK}_a$ 's of the buried sulphonic acid groups or resulted in the formation of sultones and/or intermolecular sulphonate esters. These possibilities hint at important question to be addressed by subsequent studies.

### Acknowledgements

The spent liquor from sulfite pretreatment of Douglas fir forest residuals was kindly provided by Dr. Junyong Zhu at the USDA Forest Products Laboratory (Madison, WI). This work was funded by Agriculture and Food Research Initiative Grant no. 2011-67009-20062 from the USDA National Institute of Food and Agriculture, and a Subaward (115808 G002979) from the "Northwest Advanced Renewables Alliance" led by Washington State University and supported by the Agriculture and Food Research Initiative Competitive Grant no. 2011-68005-30416 from the USDA National Institute of Food and Agriculture. X-ray powder diffraction studies and atomic force microscopy were carried out in the Characterization Facility at the University of Minnesota which receives partial support from NSF through the MRSEC program.

### References

- 1 G. Henriksson, in *Wood Chemistry and Wood Biotechnology, Pulp and Paper Chemistry and Technology*, Vol. 1, eds. M. Ek, G. Gellerstedt and G. Henriksson, de Gruyter GmbH, Berlin, 2009, pp. 121–145.
- 2 S. D. Aust, *Microb. Ecol.*, 1990, **20**, 197–209.
- 3 A. J. Ragauskas, G. T. Beckham, M. J. Biddy, R. Chandra, F. Chen, M. F. Davis, B. H. Davison, R. A. Dixon, P. Gilna, M. Keller, P. Langan, A. K. Naskar, J. N. Saddler, T. J. Tschaplinski, G. A. Tuskan and C. E. Wyman, *Science*, 2014, **344** (6185), 1246843 [DOI:10.1126/science.1246843].
- 4 J. G. Linger, D. R. Vardon, M. T. Guarnieri, E. M. Karp, G. B. Hunsinger, M. A. Franden, C. W. Johnson, G. Chupka, T. J. Strathmann, P. T. Pienkos and G. T. Beckham, *Proc. Natl. Acad. Sci. U.S.A.*, 2014, **111**, 12013–12018.
- 5 S. I. Falkehag, *Appl. Polym. Symp.*, 1975, **28**, 247–257.
- 6 A. Rezanowich and D. A. I. Goring, *J. Colloid Sci.*, 1960, **15**, 452–471.
- 7 J. F. Yan, F. Pla, R. Kondo, M. Dolk and J. L. McCarthy, *Macromolecules*, 1984, **17**, 2137–2142.
- 8 T. Saito, J. H. Perkins, D. C. Jackson, N. E. Trammel, M. A. Hunt and A. K. Naskar, *RSC Adv.*, 2013, **3**, 21832–21840.
- 9 V. P. Saraf, W. G. Glasser, G. L. Wilkes and J. E. McGrath, *J. Appl. Polym. Sci.*, 1985, **30**, 2207–2224.
- 10 Y.-r. Chen and S. Sarkanen, *Cellulose Chem. Technol.*, 2006, **40** (3-4), 149–163 and references therein.
- 11 Y. Li, J. Mlynár and S. Sarkanen, *J. Polym. Sci., B. Polym. Phys.*, 1997, **35**, 1899–1910.
- 12 J. R. Davis (ed), *Tensile Testing*, 2nd ed. ASM International, Materials Park, OH, 2004, pp. 137–154.
- 13 Y. Li and S. Sarkanen, *Macromolecules*, 2005, **38**, 2296–2306.
- 14 Y. Li and S. Sarkanen, *Macromolecules*, 2002, **35**, 9707–9715.

- 15 Y.-r. Chen and S. Sarkanen, *Phytochemistry*, 2010, **71**, 453–462.
- 16 S. Backa, M. Andersen and T. Rojahn, in *Biomass as Energy Source: Resources, Systems and Applications*, ed. E. Dahlquist, CRC Press, London, UK, 2013, pp. 141–150.
- 17 S. Sen, S. Patil and D. S. Argyropoulos, *Green Chem.*, 2015. DOI: 10.1039/C5GC01066G.
- 18 K. Lundquist, in *Methods in Lignin Chemistry*, eds. S. Y. Lin and C. W. Dence, Springer-Verlag, New York, 1992, pp. 65–70.
- 19 A. Sluiter, B. Hames, R. Ruiz, C. Scarlata, J. Sluiter, D. Templeton and D. Crocker, Technical Report NREL/TP-510-42618, National Renewable Energy Laboratory, 2011.
- 20 E. A. Capanema, M. Y. Balakshin and J. F. Kadla, *J. Agric. Food Chem.*, 2004, **52**, 1850–1860.
- 21 J.Y. Zhu, M. S. Chandra, F. Gu, R. Gleisner, R. Reiner, J. Sessions, G. Marrs, J. Gao and D. Anderson, *Bioresour. Technol.*, 2015, **179**, 390–397.
- 22 S. A. Ralph, L. L. Landucci and J. Ralph, *NMR Database of Lignin and Cell Wall Model Compounds*; <http://www.dfrc.usda.gov/software.html>, 2004.
- 23 D. Enders, N. Vignola, O. M. Berner and W. Harnying, *Tetrahedron*, 2005, **61**, 3231–3243.
- 24 Yu. L. Moreva, N. S. Alekseeva and Yu. M. Chernoberezhskii, *Russ. J. Appl. Chem.*, 2010, **83**, 1281–1283.
- 25 P. Klapetek, in *Quantitative Data Processing in Scanning Probe Microscopy*, William Andrew (Elsevier), Burlington, MA, 2013, p. 93.
- 26 C. E. Luthe, *Holzforschung*, 1990, **44**, 107–112.
- 27 S. Heikkinen, M. M. Toikka, P. T. Karhunen and I. A. Kilpeläinen, *J. Am. Chem. Soc.*, 2003, **125**, 4362–4367.
- 28 N. S. Murthy and H. Minor, *Polymer*, 1990, **31**, 996–1002.
- 29 <http://gwyddion.net/>

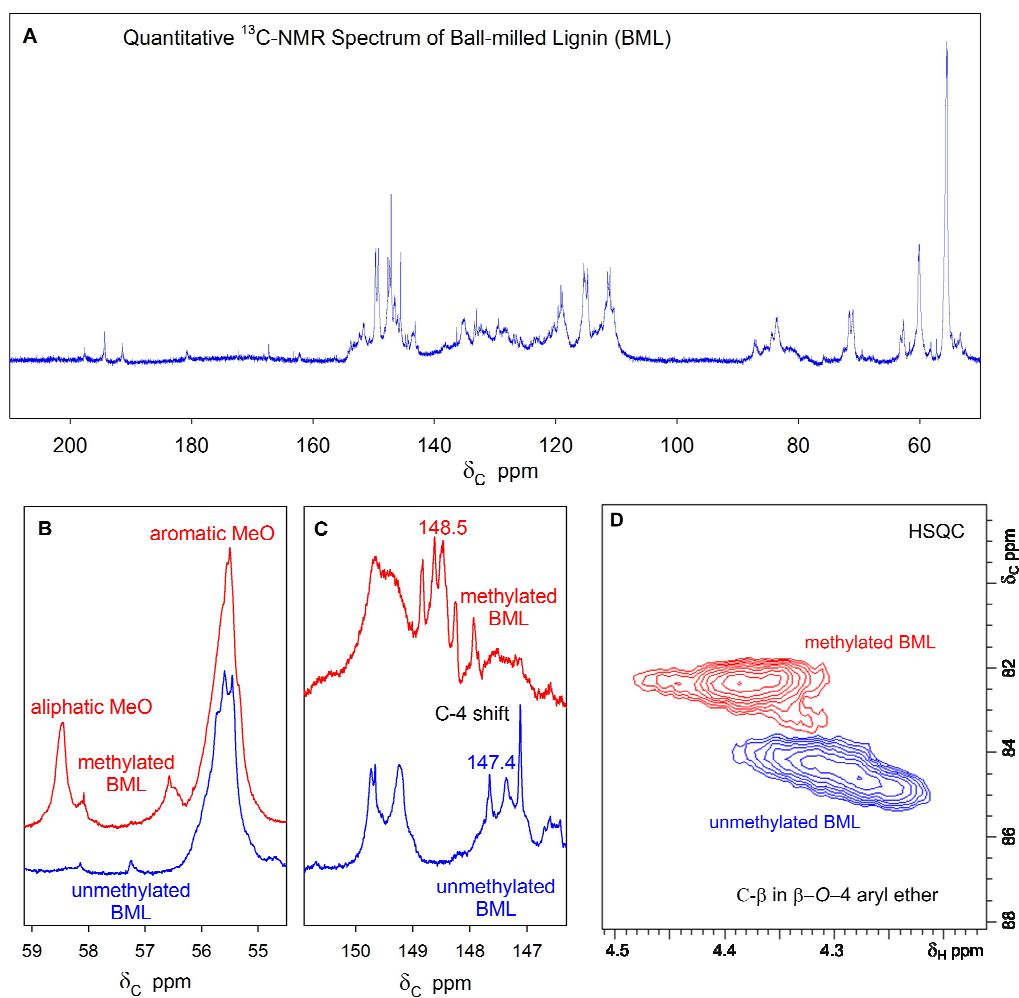


**Fig. 1** Quantitative  $^{13}\text{C}$ -NMR spectral intervals of underivatized and methylated ball-milled Jack pine lignin (BML) in  $\text{DMSO-}d_6$ . (A) 50–210 ppm interval of unmethylated BML; (B) 54.5–59 ppm interval circumscribing methoxyl region of unmethylated and methylated BML; (C) 146.5–150.5 ppm interval encompassing C-4 in unmethylated and methylated BML; (D) HSQC spectral region enclosing C- $\beta$  of alkyl aryl ether in unmethylated and methylated BML.

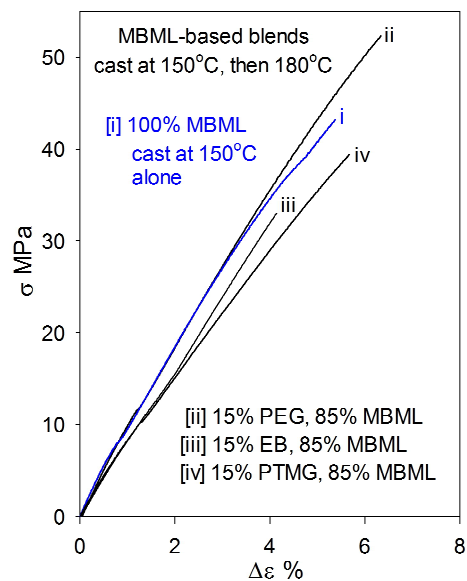


**Fig. 2** Tensile behaviour of methylated ball-milled lignin (MBML)-based polymeric materials. [i] 100% MBML-based plastic; blends of 85% MBML with [ii] 15% poly(ethylene glycol) (PEG), [iii] 15% poly(ethylene oxide-*b*-1,2-butadiene) (EB) and [iv] 15% poly(trimethylene glutarate) (PTMG).

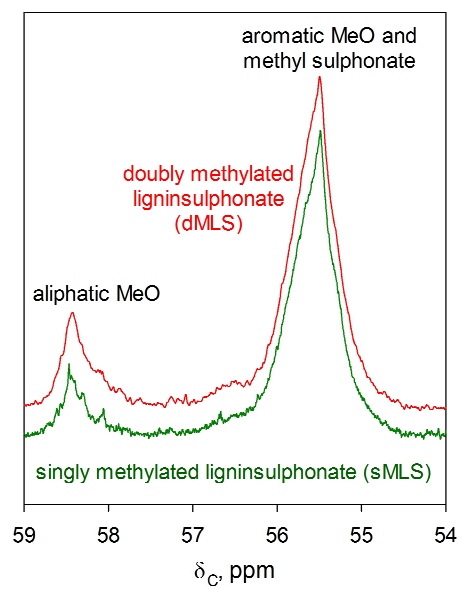


**Fig. 3** Quantitative  $^{13}\text{C}$ -NMR spectral interval circumscribing methoxyl regions of ligninsulphonate methylated with dimethyl sulphate alone (sMLS) and with dimethyl sulphate followed by diazomethane (dMLS); both derivatives in  $\text{DMSO-}d_6$ .

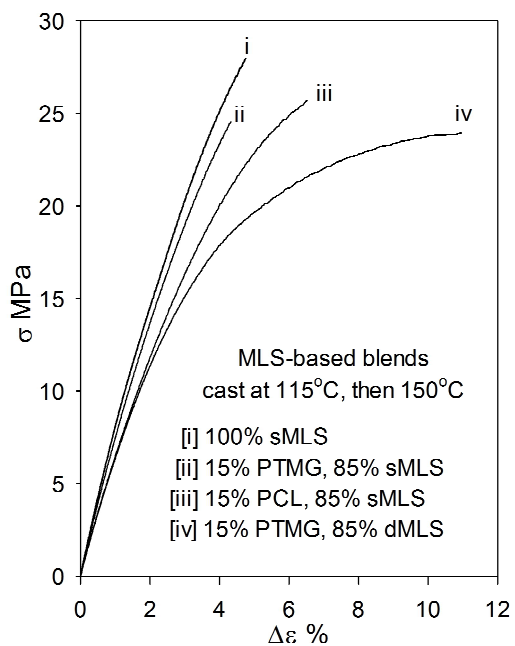


**Fig. 4** Tensile behaviour of polymeric materials based on ligninsulphonate methylated with dimethyl sulphate (sMLS) or dimethyl sulphate followed by diazomethane (dMLS). [i] 100% sMLS; blends of 85% sMLS with [ii] 15% poly(trimethylene glutarate) (PTMG) and [iii] 15% polycaprolactone (PCL); [iv] blend of 85% dMLS with 15% PTMG cast stepwise at 115°, 125°, 135° and then 150°C.

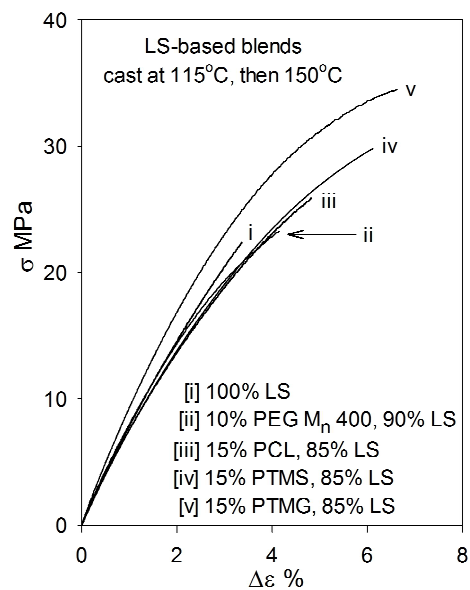


**Fig. 5** Tensile behaviour of ligninsulphonate (LS)-based polymeric materials. [i] 100% LS; [ii] blend of 90% LS with 10% PEG,  $M_n$  400 Da; blends of 85% LS with [iii] 15% polycaprolactone (PCL), [iv] 15% poly(trimethylene succinate) (PTMS), and [v] 15% poly(trimethylene glutarate) (PTMG).

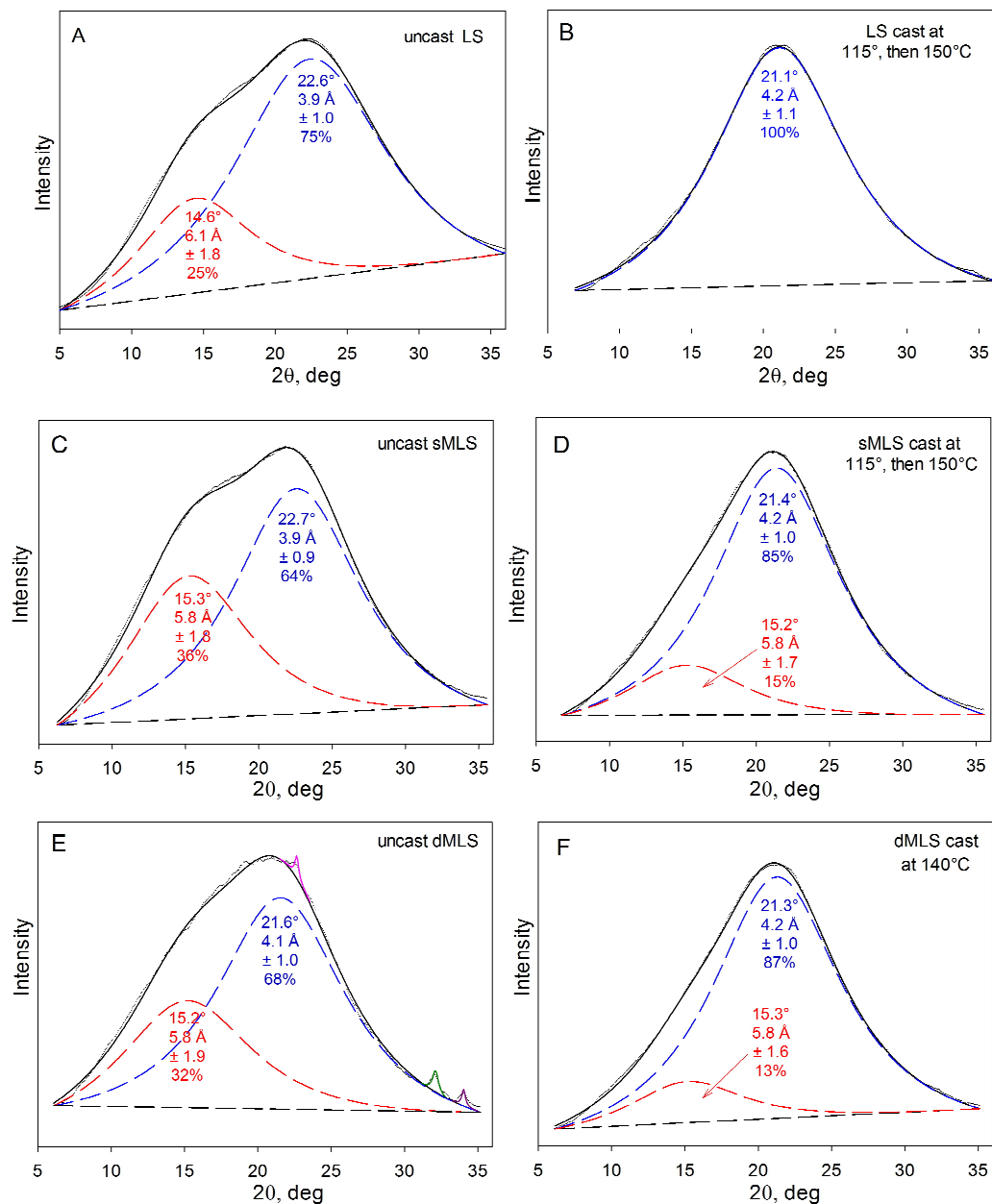


**Fig. 6** X-ray powder diffraction patterns of uncast and cast polymeric materials based on unmodified and methylated ligninsulphonates. (A) uncast and (B) cast unmodified ligninsulphonate (LS); (C) uncast and (D) cast ligninsulphonate methylated with dimethyl sulphate (sMLS); (E) uncast and (F) cast ligninsulphonate successively methylated with dimethyl sulphate and diazomethane (dMLS). The x-ray diffraction patterns of the amorphous polymeric materials were analysed by fitting two Lorentzian functions  $I(x) = I(0)/(1 + x^2/hw^2)$ ,  $x = 2\theta - 2\theta_k$ , where  $I(x)$  is the scattered intensity at  $x$  from the Bragg angle  $2\theta_k$  for the peak,  $2\theta$  is the scattering angle, and  $hw$  is the half-width at the half-maximum of the peak.



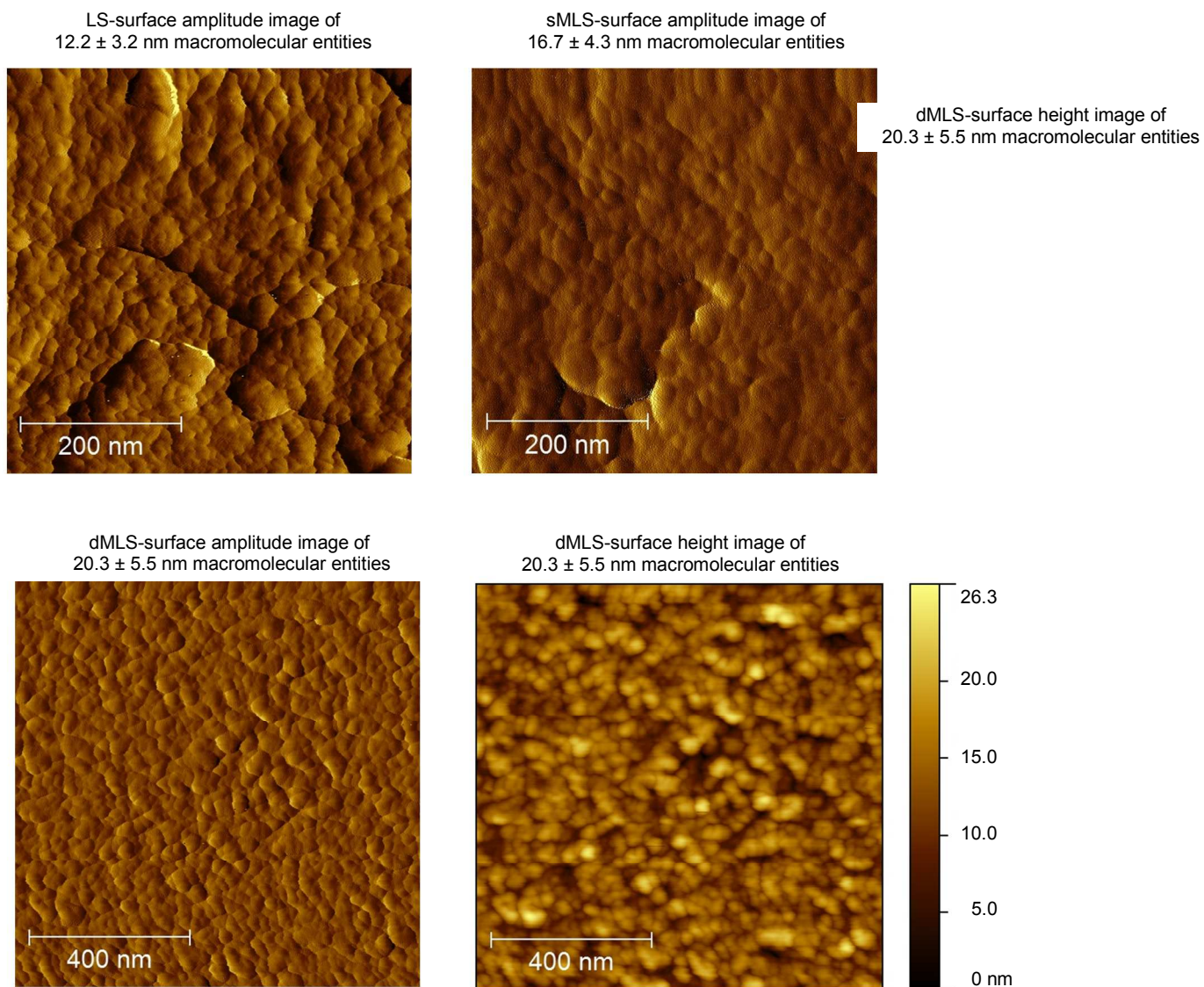


**Fig. 7** Packing of macromolecular entities in ligninsulphonate (LS)-based polymeric materials cast at  $115^\circ$  and then  $150^\circ\text{C}$ . Tapping-mode AFM amplitude images of ultramicrotome-cut surfaces of (A) unmethylated LS, (B) LS methylated with dimethyl sulphate (sMLS), (C) LS successively methylated with dimethyl sulphate and diazomethane (dMLS); (D) corresponding height image of dMLS surface (material cast stepwise at  $115^\circ$ ,  $125^\circ$  and  $150^\circ\text{C}$ ).

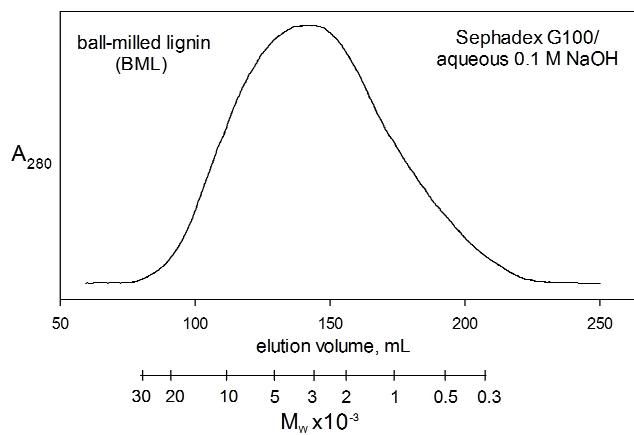


**Fig. 8** Molecular weight distribution of ball-milled Jack pine lignin ( $M_w = 4300$ ,  $M_n = 1850$ ). Aqueous 0.1 M NaOH/Sephadex G100 elution profile calibrated by paucidisperse poly(styrene sulphonate) fractions.

In tensile behaviour, polymeric materials containing only methylated ball-milled lignin surpass polystyrene, while 85% w/w ligninsulphonate blends approach polyethylene.